PCCP

RSC Publishing

PAPER

View Article Online
View Journal | View Issue

Cite this: *Phys. Chem. Chem. Phys.*, 2013, **15**, 14986

Molecular rheometry: direct determination of viscosity in L_o and L_d lipid phases *via* fluorescence lifetime imaging†

Yilei Wu,‡[a] Martin Štefl,‡[bc] Agnieszka Olzyńska,[b] Martin Hof,[b] Gokhan Yahioglu,[d] Philip Yip,[be] Duncan R. Casey,[a] Oscar Ces,[a] Jana Humpolíčková*[b] and Marina K. Kuimova*[a]

Received 8th May 2013,
Accepted 9th July 2013

DOI: 10.1039/c3cp51953h

www.rsc.org/pccp

Understanding of cellular regulatory pathways that involve lipid membranes requires the detailed knowledge of their physical state and structure. However, mapping the viscosity and diffusion in the membranes of complex composition is currently a non-trivial technical challenge. We report fluorescence lifetime spectroscopy and imaging (FLIM) of a *meso*-substituted BODIPY molecular rotor localised in the leaflet of model membranes of various lipid compositions. We prepare large and giant unilamellar vesicles (LUVs and GUVs) containing phosphatidylcholine (PC) lipids and demonstrate that recording the fluorescence lifetime of the rotor allows us to directly detect the viscosity of the membrane leaflet and to monitor the influence of cholesterol on membrane viscosity in binary and ternary lipid mixtures. In phase-separated 1,2-dioleoyl-*sn-glycero*-3-phosphocholine-cholesterol–sphingomyelin GUVs we visualise individual liquid ordered (L_o) and liquid disordered (L_d) domains using FLIM and assign specific microscopic viscosities to each domain. Our study showcases the power of FLIM with molecular rotors to image microviscosity of heterogeneous microenvironments in complex biological systems, including membrane-localised lipid rafts.

Introduction

Physical parameters of lipid membranes, such as lateral lipid diffusion, stiffness, hydration and viscosity, have a fundamental impact on many membrane-associated cellular processes, such as lipid and protein sorting.[1] However, mapping these parameters with high spatial resolution presents significant challenges. Among the most commonly used non-invasive approaches in the characterization of membrane diffusion are fluorescence recovery after photobleaching (FRAP),[2] single particle tracking (SPT)[3] and several techniques derived from fluorescence correlation spectroscopy (FCS).[4] In spite of the fact that several technically-demanding FCS-based techniques, such as imaging total internal reflection FCS,[5] or single plane illumination microscopy FCS,[6] are able to generate maps of diffusion coefficients, in the majority of cases only a single-spot readout is possible and spatially-resolved information is inaccessible.

Molecular rotors[7–11] represent a promising tool for monitoring microscopic viscosity, which combines speed of acquisition with the availability of spatially-resolved information and imaging capability. Since viscosity is the major parameter which controls the speed of diffusion in condensed media, including that of lipids and proteins in membranes,[12] the molecular rotor approach can provide valuable complementary information on diffusion in biological systems, which is unavailable when using any other currently existing spectroscopic techniques.

In molecular rotors the non-radiative deactivation rate responds strongly to the viscosity of their immediate environment.[9,11] This typically occurs as a result of a viscosity-dependent intramolecular structural change, such as twisting or rotation, which is coupled to a population of the dark non-emissive electronic excited state(s). For example, intramolecular rotation in the 9-(dicyanovinyl)julolidine (DCVJ)[9] leads to a population of the 'dark' twisted intramolecular charge transfer (TICT) excited state, leading to a reduced fluorescence.

[a] *Department of Chemistry, Imperial College London, Exhibition Road, London, SW7 2AZ, UK. E-mail: m.kuimova@imperial.ac.uk*
[b] *J. Heyrovsky Institute of Physical Chemistry, Academy of Sciences of the Czech Republic, Prague 8, 182 23, Czech Republic. E-mail: jana.humpolickova@jh-inst.cas.cz*
[c] *Department of Biochemistry, Faculty of Science, Charles University, Prague 2, 128 43, Czech Republic*
[d] *PhotoBiotics Ltd, 21 Wilson Street, London EC2M 2TD, UK*
[e] *Department of Physics, SUPA, University of Strathclyde, Glasgow G4 0NG, Scotland, UK*

† Electronic supplementary information (ESI) available: Additional spectroscopic data. See DOI: 10.1039/c3cp51953h

‡ These authors contributed equally.

The immediate consequence of the viscosity-dependent intramolecular rotation is the sharp increase in both the fluorescence quantum yield (Φ_f) and the fluorescence lifetime (τ_f) as a function of the increasing viscosity (η).[11] The calibration plot of fluorescence parameters *versus* viscosity can be created based on the Förster–Hoffmann equation:[13]

$$\Phi_f = z\eta^{\alpha} \quad (1)$$

where z and α are constants.

The main problem of the steady-state approach using the quantum yield of molecular rotors is the inability to distinguish between viscosity and other factors which might affect the fluorescence intensity, such as the local dye concentration. A ratiometric approach, removing the uncertainties in the probe concentration, has been used to solve this problem.[10,14]

Alternatively, it is possible to exploit the dependence of fluorescence lifetime of molecular rotors on viscosity:

$$\tau_f = zk_r^{-1}\eta^{\alpha} \quad (2)$$

where k_r is a radiative decay constant.

The fluorescence lifetime is independent of the fluorophore concentration, in the absence of self-quenching and/or aggregation. In addition, it is possible to utilise fluorescence lifetime imaging (FLIM) of molecular rotors in order to obtain maps of viscosity in heterogeneous environments.

Heterogeneities in membrane organisation are a highly discussed topic in cell biology. In this study we utilise the strong dependence of fluorescence lifetime of the *meso*-substituted boron–dipyrrin dye, *m*-phenyl–BODIPY (Scheme 1D), on the viscosity of the local environment to measure membrane fluidity. We incorporate molecular rotors into model lipid bilayers and measure the bilayer viscosity under a variety of conditions. Importantly, we are able to measure viscosity in pure or mixed lipid systems and image viscosity in the phase-separated domains using FLIM.

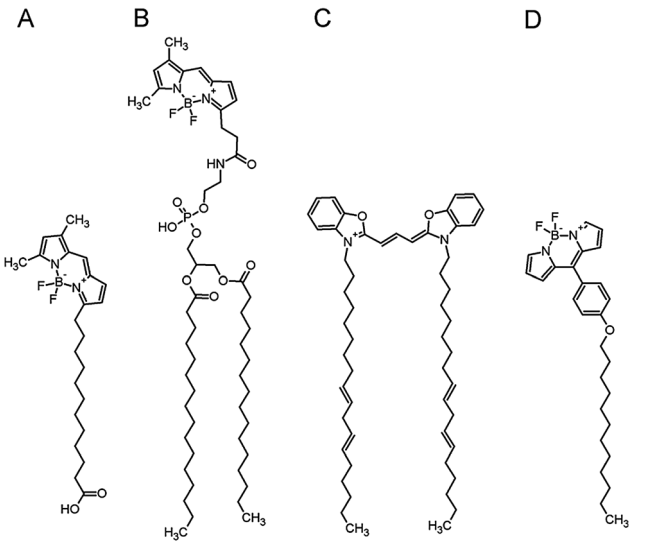

Scheme 1 Structures of the labelled lipids–lipid tracers used in this study: (A) BODIPY-FL-C_{12}, (B) BODIPY-FL-DHPE, (C) $DiOC_{18}$, (D) BODIPY rotor.

Materials and methods

The *meso*-substituted BODIPY dyes with either the $-C_{10}$ or the $-C_{12}$ aliphatic chains (Fig. S1, ESI†) were synthesised as described elsewhere.[8] 1,2-Dilauroyl-*sn-glycero*-3-phosphocholine (DLPC), 1,2-dimyristoyl-*sn-glycero*-3-phosphocholine (DMPC), 1,2-dipalmitoyl-*sn-glycero*-3-phosphocholine (DPPC), 1,2-dioleoyl-*sn-glycero*-3-phosphocholine (DOPC), 1-palmitoyl-2-oleoylphosphatidylcholine (POPC), porcine brain sphingomyelin (Sph), cholesterol, 1,2-dioleoyl-*sn-glycero*-3-phosphoglycerol (DOPG), and 1,2-dipalmitoyl-*sn-glycero*-3-phosphoethanolamine *N*-(cap biotinyl) (Biotinyl Cap PE) were purchased from Avanti Polar Lipids (Alabaster, AL). Bodipy® FL DHPE, BODIPY® FL C12, $DiO\Delta^{9,12}$-C_{18}(3) (DiO) were purchased from Invitrogen (Carlsbad, CA). Streptavidin, biotin labelled bovine serum albumin (biotin-BSA) were purchased from Sigma (St. Louis, MO).

Preparation of GUVs and LUVs

GUVs were prepared by a gentle hydration approach described elsewhere.[15] 1 mL of lipid mixture in chloroform containing 1 mg of lipid was dried with a rotary evaporator and kept for additional two hours under vacuum. Lipid films were hydrated with 3 mL of pre-warmed buffer (10 mM HEPES, 150 mM NaCl, 1 mM $CaCl_2$, 0.1 M sucrose, pH = 7) saturated with nitrogen. The tube was then sealed, heated to 60 °C overnight, and then slowly cooled. The white cloudy suspension of liposomes was gently vortexed before further use. The lipid mixtures contained 5 mol% of DOPG, a negatively charged lipid, and 4 mol% of biotinyl Cap PE necessary for attaching GUVs to BSA-biotin–streptavidin coated glass. All the measurements on GUVs were performed in an FCS2 chamber (Bioptechs, Butler, PA). The chamber with a coated coverslip was filled with 200 μL buffer solution (10 mM HEPES, 150 mM NaCl, 1 mM $CaCl_2$, 0.1 M glucose, pH = 7), then 20 μL of the solution containing GUVs was added and incubated for 30 minutes after which the chamber was carefully flushed with an excess of the buffer solution to remove unattached GUVs.

For LUV formation, the appropriate lipid mixture containing 10^{-7} mol of lipid and 10^{-10} mol of BODIPY was prepared in chloroform. The chloroform was evaporated using a rotary evaporator and the lipid film re-hydrated with 1 mL of pre-heated (60 °C) buffer solution (10 mM HEPES, 150 mM NaCl, 2 mM EDTA, pH = 7). The turbid solution containing multilamellar vesicles was extruded 10 times using 200 nm filters in a LIPEX extruder (Northern Lipids Inc., Canada).[16] The extrusion was carried out above the fluid-gel transition temperature of all lipids in the mixture.

Time correlated single photon counting (TCSPC)

TCSPC measurements were performed on bulk cuvette samples (LUVs) and on the microscope stage using FLIM (GUVs). The bulk fluorescence lifetime measurements were performed using a HORIBA Jobin Yvon IBH 5000F time-correlated single-photon counting device equipped with a monochromator, by using a pulsed NanoLED excitation source at 467 nm (IRF *ca.* 300 ps). Low absorption was maintained at the excitation wavelength (A = 0.1).

FLIM measurements were performed on a MicroTime 200 inverted confocal microscope (PicoQuant, Germany) with a water immersion objective (1.2 NA, 60×, Olympus). A pulsed diode laser (LDH-P-C-470, 470 nm, PicoQuant) with a 40 MHz repetition rate was used for excitation. The fluorescence signal was focused on a 50 μm pinhole and detected by a single photon avalanche diode (Perkin-Elmer SPCM-AQR) using a 515/50 emission filter (Chroma). The intensity of the lasers was chosen so as to avoid pile-up effect (1 μW). Each GUV was scanned in the cross-section, and an image of 512 × 512 pixels (0.6 ms per pixel) was acquired.

2-Foci FCS measurements

2fFCS experiments were carried out on the home built confocal microscope[17] consisting of an inverted confocal microscope body IX71 (Olympus). For excitation, the 60 ps pulsed 470 nm diode laser head LDH-P-C-470B (Picoquant) was used. The polarisation of the laser light was periodically rotated using an electro-optic amplitude modulator (EO-AM-R-20-C4, Thorlabs) such that the polarisation of every pulse was orthogonal with respect to the previous one. The laser pulses were synchronised with the sine voltage wave imposed on the modulator using a DA4300 30 MS/s arbitrary waveform generator (Acquitek). The voltage output was further amplified.

The laser light was coupled to the single mode optical fiber (in which polarisation was maintained) and re-collimated at the output with an UPlanSApo 10× N.A. 0.4 objective lens (Olympus) so that the beam light under-filled the principal microscope objective lens (60×, W, 1.2 N.A., Olympus) and the size of the focal spot was enlarged compared to the diffraction limited case. The light was reflected up to the objective with a Z470rdc dichroic mirror (Chroma). Underneath the objective lens, a Nomarkski prism (U-DICTHC, Olympus) was placed such that its axes were aligned with the orthogonal polarisation of the laser pulses. Thus the pulses of different polarisations were focused onto two spatially shifted, overlapping foci. The distance between the foci was precisely determined by scanning of sub-diffraction sized fluorescence beads.

The emission light was focused on a 150 μm pinhole and after re-collimation split on the two single-photon avalanche diodes (Micro-Photon Devices, Bolzano, Italy) with emission filters (HQ515/50).

The auto- and cross-correlation functions (ACFs, CCFs) corresponding to the fluorescence intensity traces in the individual foci were calculated and fitted in Matlab (Mathworks, Natick, MA) using custom scripts that take into account the point spread function (PSF) and the mathematical model of 2-dimensional diffusion described by Dertinger *et al.*[18]

Results and discussion

Temperature and composition effect on the rotor calibration

The Förster–Hoffmann calibration graph of fluorescence lifetime *versus* viscosity for BODIPY is given in Fig. 1. We performed calibration in methanol–glycerol mixtures, where viscosity can be altered in a very wide range (0.5–5000 cP) by both the solvent mixture composition and the temperature. We reasoned that using both the temperature and the composition of the mixture interchangeably would deliver the most precise calibration graph possible, Fig. 1.

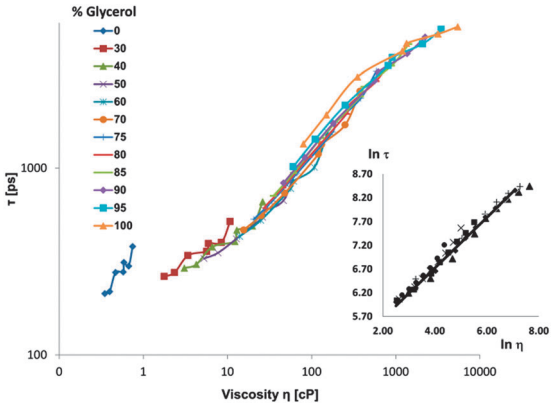

Fig. 1 Fluorescence lifetime of BODIPY recorded in methanol–glycerol mixtures of various compositions, plotted against viscosity. The data were taken at temperatures between 278 and 334 K. Inset: the linear plot of $\ln\tau$ *vs.* $\ln\eta$ (Förster–Hoffmann equation) for mixtures between 40 and 95% glycerol.

From these data we were able to draw the following conclusions: firstly, the fluorescence lifetime of BODIPY molecular rotor follows the Förster–Hoffmann equation between 10 cP ($\ln\eta$ = 2.3) and 4500 cP ($\ln\eta$ = 8.4), since a good linear correlation is observed between $\ln\tau$ and $\ln\eta$ in this range, Fig. 1 (inset).

Secondly, the temperature increase does not affect the photophysics of BODIPY or its function as a molecular rotor, apart from changing the viscosity of the solvent. This is consistent with the low activation energy reported for a similar compound.[19] Importantly, our results indicate that the BODIPY rotor is suitable for direct viscosity measurements in lipid membranes at variable temperatures.

Viscosity measurements in lipid bilayers: single lipid LUVs

Previously, the BODIPY rotor was used for viscosity measurements in the membranes of vesicles of live cells.[7,8] Here, we set out to investigate the viscosity of a lipid bilayer system where more precise control of the membrane properties is possible. To do so, we measured fluorescence lifetimes of BODIPY, incorporated into single-lipid artificial bilayers, prepared as LUVs. LUVs of 200 nm diameter were constructed from saturated PC lipids with hydrocarbon chains of different lengths: DLPC (C_{12}), DMPC (C_{14}), DPPC (C_{16}) and unsaturated C_{18} lipids: POPC (a single *cis*-double bond in the C_9 position) and DOPC (both chains containing a *cis*-double bond in the C_9 position).

These lipids are characterised by different gel-to-liquid (L_β to L_α) transition temperatures, which increase with increasing length of the hydrocarbon chains. Importantly, the transition temperature decreases dramatically for unsaturated lipids, *e.g.* $T_{DOPC} = -20$ °C. Such low transition temperatures ensure that membranes in live cells, containing unsaturated lipids, can remain fluid at room temperature. This is considered essential for signal transduction, transport and the necessary interactions

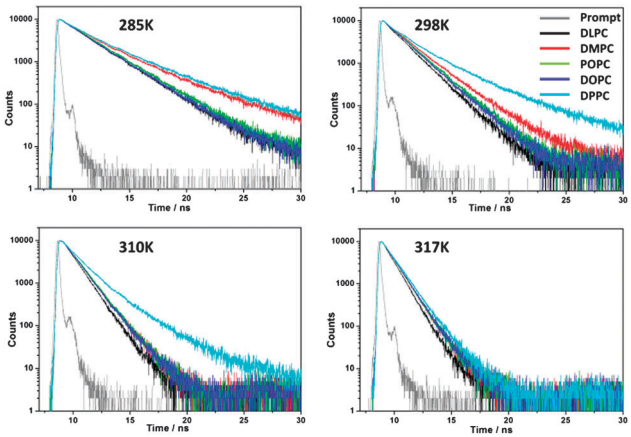

Fig. 2 Time-resolved fluorescence decay traces of BODIPY embedded in five PC lipids at 285 K, 298 K, 310 K and 317 K. The instrument response function is also shown.

and reactions within cells and, in particular, within the plasma membrane.

Initially we investigated a range of BODIPY concentrations in LUVs and concluded that [lipid]:[dye] ratios between 400 and 800 are optimal for viscosity measurements in bilayers. At higher ratios, low fluorescence signals are observed, which dramatically lengthen observation times. At significantly lower ratios (*e.g.* 80 : 1 [lipid]:[dye]) there is strong evidence of dye–dye interactions inside the bilayer, leading to biexponential emission decays and excited state quenching. An example of a spectral study of DOPC LUVs containing 20 : 1 [lipid]:[dye] is given in the ESI† (Fig. S2 and S3).

Following the optimisation of the lipid/dye ratios, the time-resolved fluorescence decay traces of BODIPY inside lipid bilayers were recorded between 285 and 345 K to test the effect of temperature on the bilayer viscosity, Fig. 2. It could be clearly seen that the time-resolved fluorescence decay traces of the BODIPY rotor inside lipid bilayers change shape as a function of temperature.

Most notably, below the transition temperature (in the gel phase) the decays are biexponential in all cases, *e.g.* see DPPC and DMPC at 285 K, Fig. 2. We have also monitored the fluorescence intensity of BODIPY in DPPC as a function of temperature, Fig. 3, and confirmed that we can clearly observe the gel-to-liquid phase transition at 41 °C, by the change of the gradient of the '*Intensity*(*T*)' plot.

Since biexponential decays can be evidence of BODIPY aggregation (see Fig. S2 and S3, ESI†), we have performed tests to ensure that in the gel phase, below the transition temperature of DPPC there were no spectroscopic signatures of red emitting BODIPY aggregates, Fig. S4 and S5 (ESI†). While based on this data we cannot exclude the formation of 'dark' non-emissive aggregates, we believe this is unlikely given the high lipid : dye ratios in these experiments, from 400 : 1 to 800 : 1. Thus we assigned the two fluorescence lifetimes detected for BODIPY in the gel phase to different viscosity/rigidity environments, experienced by a fluorophore in the gel phase, rather than aggregation. Our lifetime measurements give viscosities of *ca.* 160 cP (1.5 ns, 50%) and

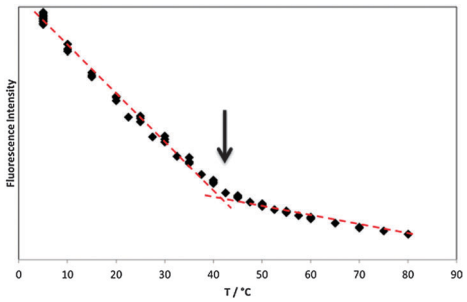

Fig. 3 The temperature dependence of the steady-state fluorescence intensity of BODIPY in 200 nm LUVs constructed from DPPC. The transition temperature of DPPC (41 °C) is also shown, determined by the intersection of the intensity *versus* temperature plots below and above the transition temperature.

1300 cP (4.5 ns, 50%). These high values are consistent with the known high rigidity of gel phases. The lower viscosity of *ca.* 160 cP may reflect the different positioning of the fluorophore in a bilayer. We note that it is likely that many more than just two kinds of environments, with viscosities between 160 to 1300 cP exist in a bilayer in the gel phase, although it is possible to fit the data using a biexponential model. Multiple localisations of chromophores in the DPPC gel phase have been previously demonstrated for other membrane labels,[20] consistent with our results.

In contrast to the gel phase bilayers, monoexponential decays of the BODIPY rotor were consistently observed in liquid disordered (L_d) phase LUVs, characteristic of a single fluorophore environment. We have used the Förster–Hoffmann calibration graph, Fig. 1, to convert the lifetimes to viscosities of each bilayer composition, across a range of temperatures.

The analysed data are given in Fig. 4 and the viscosity scale is shown as a separate axis. An Arrhenius-type dependence is observed in the data: however, the variation in the 'activation energies' thus obtained (Fig. S6, ESI†) might not be very meaningful, given that it could arise from a temperature sensitivity of either the radiative or the non-radiative rate constants of BODIPY, as well as its sensitivity to a bilayer viscosity (*via* k_{nr}).

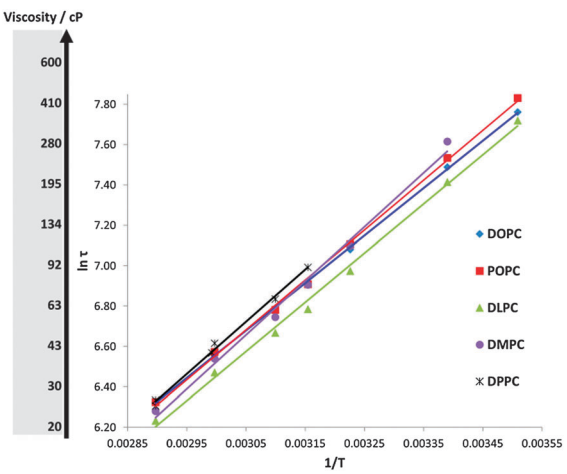

Fig. 4 The lifetime and viscosity variations in LUVs constructed of five PC lipids with temperature, plotted in Arrhenius coordinates.

Importantly, the viscosity values obtained for L_d phase bilayers at room temperature and at 37 °C (cell culture temperature) are between 100 and 300 cP, consistent with the data obtained with the same molecular rotor for membranes of vesicles in live cells.[7,8] This confirms our hypothesis that BODIPY targets the lipid-bilayer domains of cellular organelles. These data demonstrate the great potential of the BODIPY molecular rotor and its derivatives for viscosity studies in microenvironments of live cells.

Binary lipid mixtures, cholesterol sensing

The presence of cholesterol is essential for many membrane-associated processes.[21] It is also well known that cholesterol affects membrane properties such as lateral lipid diffusion.[22] We have prepared large unilamellar vesicles (LUVs) containing either DOPC or sphingomyelin with varying amounts of added cholesterol and used BODIPY to directly determine their viscosities.

Fig. 5 shows that there is a significant difference between the decays observed in DOPC- and sphingomyelin-containing LUVs. These differences arise due to the different phases of the lipids. While the DOPC bilayer is in the fluid phase at room temperature, the Sph bilayer is expected to be in the gel phase. Thus, the overall decay of BODIPY in Sph bilayers is significantly longer than in DOPC. In addition, the decays observed in Sph require biexponential fitting, consistent with the data observed for DPPC and DMPC below their transition temperatures, Fig. 2.

While the difference between the binary mixtures DOPC–Chol and Sph–Chol is substantial, the effect of the addition of cholesterol within each mixture appears to be minor, yet significant. For DOPC–Chol (in the fluid phase) the lifetime of the rotor increases from 1.78 ± 0.05 to 1.92 ± 0.05 ns (228 to 263 cP) upon addition of 40% cholesterol. Thus for the increased cholesterol content we measure an increase in the membrane viscosity by approximately 16%.

We have performed 2fFCS measurements of the BODIPY diffusion coefficient in free-standing phospholipid bilayers in giant unilamellar vesicles (GUVs) in order to correlate the change in viscosity with changes of the lateral diffusion coefficient, Table 1. It can be seen that the diffusion coefficient of the BODIPY rotor decreases by about 42% upon addition of 40% cholesterol to DOPC. A similar drop in the diffusion coefficient, of *ca.* 30%, in DOPC–Chol bilayers was also shown by Kahya *et al.*[4] Thus, in our case, the viscosity increase measured using molecular rotors appears to be smaller than the drop in the value of the diffusion coefficient.

Table 1 Diffusion coefficients of the molecular rotor in the DOPC–Chol membranes measured in the GUVs by means of two-foci FCS

DOPC–Chol [mol%]	100/0	75/25	60/40
D [μm^2 s^{-1}]	14.6	11.4	8.4
StDev [μm^2 s^{-1}]	1.2	1.4	0.5
N^a	6	8	7

[a] The number of measurements performed.

In a system of spherical symmetry, the diffusion coefficient D is related to the viscosity by the following formula:

$$D = \frac{kT}{6\pi\eta R} \quad (3)$$

where k is Boltzmann's constant, T is absolute temperature and R is the hydrodynamic radius.

This equation predicts that the relative viscosity change should be equal to the relative change in the diffusion coefficient, which apparently does not hold in our case. However, it has to be emphasised that viscosity in highly anisotropic systems, such as membranes is not trivial to interpret. For example, membrane inclusions such as individual lipid molecules, peptides or proteins, experience different viscosities in the membrane plane (η) and in contact with the outer liquid (η'). For such an inclusion the use of the Saffman–Delbrück formula is more appropriate.[23]

$$D = \frac{kT}{4\pi\eta h}\left(\ln\frac{\eta h}{\eta' R} - \gamma\right) \quad (4)$$

where h is the thickness of the bilayer, R is the radius of the embedded cylindrical inclusion and γ is Euler's constant.

Thus, in addition to the membrane viscosity, the membrane thickness will have an impact on the diffusion coefficient. For example, if $\eta h \sim 4 \times 10^{-10}$ Pa s m,[11] $\eta' = 1 \times 10^{-3}$ Pa s and $R \sim 1$ nm, $h = 4$ nm, the relative change in viscosity by 16% would require around 26% change in the membrane thickness to account for the entire change of the diffusion coefficient. For the DOPC bilayer, an increase in membrane thickness by approximately 8% was reported.[24] Thus the BODIPY-reported viscosity change does not fully account for the change in D. This might be due to the following reasons: (i) the rotor might not be optimally localized to sense the friction among adjacent moving lipid molecules. Indeed, a bilayer is an anisotropic system. While the dimensions of the rotor are small and it is fully embedded in the tail region of the bilayer it is possible that its rotational axis is not perpendicular to the bilayer plain. If so, the intramolecular motion of the rotor responsible for the viscosity sensitivity might not reflect the molecular friction in

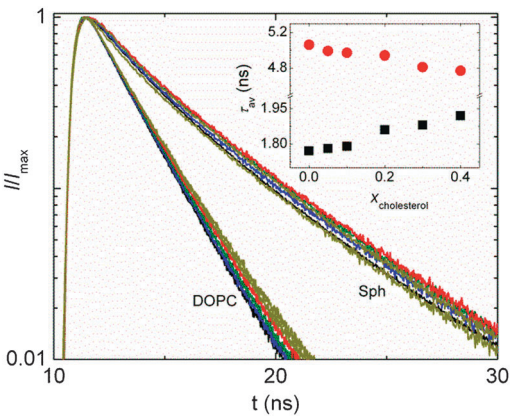

Fig. 5 Time-resolved fluorescence decay traces of BODIPY in the DOPC–Chol and Sph–Chol mixtures containing 0% (black), 5% (blue), 10% (green), 20% (red), 30% (orange), and 40% (dark yellow) cholesterol. Inset: dependence of the monoexponential fluorescence lifetime (in DOPC, ■) and the long-lifetime decay component (Sph, ●) on the cholesterol content.

the bilayer, and the rotor read-out for a 2D system (membrane) can differ from that of a 3D system (calibration mixtures). Alternatively (ii) the Saffman–Delbrück formula might not be an ideal mathematical description for the membrane-inserted probe as it assumes a cylindrical trans-membrane inclusion.

In the case of sphingomyelin bilayers, a biexponential decay analysis is required to fit the data. Upon addition of up to 40% cholesterol the short lifetime component (*ca.* 2 ns) experiences little change, while the long component decreases from 5.1 ± 0.1 ns to 4.8 ± 0.1 ns (see Fig. 5, inset). This corresponds to an approximately 10% decrease in viscosity (from 1620 to 1450 cP), which is a reasonable impact of cholesterol on the fluidity of the sphingomyelin rich membrane, most probably reporting a gradual change of gel phase into the L_o phase.[25] However, it has to be emphasised that the presence of the short component (due to a differently localised dye fraction) decreases the robustness of the lifetime analysis in this case.

Ternary lipid mixtures, cholesterol sensing and phase co-existence

We were keen to use the molecular rotor BODIPY to investigate the viscosity of a phase-separated system. Thus we investigated the viscosity in GUVs made up of DOPC–Sph–Chol. In this ternary mixture at certain compositions (see the phase diagram in Fig. 6b), phases can be optically resolved and fluorescence lifetime imaging (FLIM) of BODIPY can be used to visualise the viscosity directly in the phase of interest.

No phase separation was observed for mixtures containing 5% DOPC/(55–95)% Sph/(0–40)% Chol, however, the effect of increased cholesterol concentration could be detected by monitoring the fluorescence lifetime of the rotor, Fig. S7 (ESI†). Likewise, for mixtures containing fixed 5% Sph/(55–95)% DOPC/(0–40)% Chol, we detected the changes in the BODIPY lifetime, associated with [Chol] increase, Fig. S7 (ESI†).

Next, we have recorded BODIPY time-resolved fluorescence decays in GUVs composed of mixtures containing 25% cholesterol with varying ratios of DOPC and Sph. These mixtures are represented by the green line on the ternary phase diagram, shown in Fig. 6, adopted from Smith *et al.*[26]

This diagram describes changes in lipid compositions of individual phases in the two-phase coexistence region when the overall lipid composition is altered along the green line. The fluorescence decays are discussed along three different lines: (i) between the points A and B corresponding to the one-phase region (L_d), (ii) between the points B and C, where all the investigated lipid compositions were in the L_d phase in the two phase region, and (iii) between the points B and D, where the investigated experimental compositions were in the L_o phase in the two phase region.

The inspection of the decay curves collected for compositions between points A and B, Fig. 6 (left), shows no detectable lifetime change, which suggests that the membrane viscosity is either not affected by the increased amount of Sph, or its changes are below the resolution limit of our approach. The decays collected from the L_d phase in the two phase region between points B and C, do not show a significant change until 50% of Sph is reached, when the long lifetime component (around 90% amplitude) increases from 2.3 to 2.6 ns, which corresponds to *ca.* 28% increase in membrane viscosity, from 370 to 465 cP. Similarly, there are no significant lifetime changes in the L_o phase until *ca.* 40% of Sph, when a lifetime increase becomes apparent, Fig. 6c. The overall increase of the long lifetime component from 3.0 ns (20% Sph) to 3.5 ns (60% Sph) corresponds to almost 36% increase in viscosity, 600 to 810 cP.

The images of GUVs in the two phase region, revealed two phases which differed both in the intensity and in the fluorescence lifetime, Fig. 7. The corresponding decays collected from the L_d and L_o phases give lifetimes of 2.3 ns and 3.5 ns, respectively, which correspond to viscosities of 370 cP and 810 cP. To the best of our knowledge this is the first direct viscosity measurement in the L_o phase, which is reminiscent of lipid rafts. As expected, our measurements demonstrate that the L_o phase has a very high viscosity.

It is very clear from our data (Fig. 7) that it is possible to distinguish between the L_o and L_d phases on the basis of the BODIPY lifetime in the bilayer and to measure the viscosity of these phases directly. However, we note the lack of rotor affinity for the higher ordered phases, which can decrease its usefulness for sensing the L_o phase, especially in live cells. Inspection of the

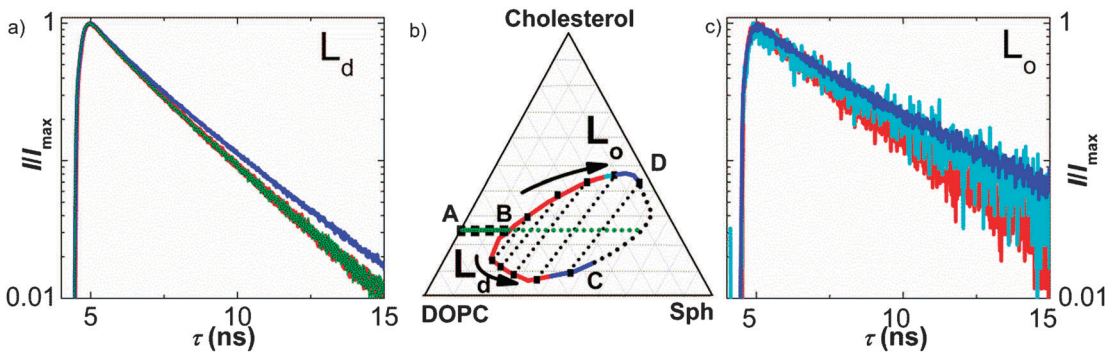

Fig. 6 Time-resolved fluorescence decays of BODIPY recorded in DOPC–Sph–Chol GUVs of varying composition. Left: decays recorded in the L_d phase in the single-phase region: A to B (green), and in the two-phase mixtures, B to C (red and blue). Right: decays recorded in the L_o phase in the two-phase region: B to D (red – light blue – dark blue). The phase diagram for the ternary system DOPC–Sph–Chol, adapted from ref. 26, is also shown.

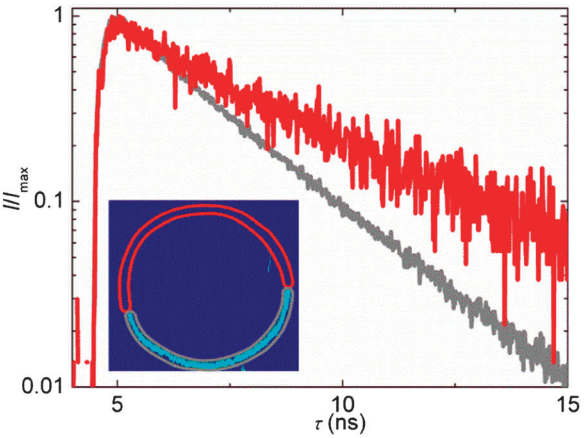

Fig. 7 Time-resolved fluorescence decays of BODIPY recorded in DOPC–Sph–Chol GUV (35 : 40 : 25 composition) in the L_d phase (grey) and in the L_o phase (red). Inset: cross-sectional image of the GUV, pixels marked in red and blue correspond to the L_o and L_d phases, respectively.

GUVs in the phase coexistence region suggests considerably higher affinity for the L_d phase ($K_D = 19 \pm 1$ at the composition DOPC/Sph/Chol = 35/40/25). For FLIM viscosity measurements of GUVs, when ordered domains can be detected and analysed individually, this lack of affinity does not present any problem. However, when trying to detect the viscosity of elusively small domains in live cells (*e.g.* lipid rafts), possibly of the size below the resolution limit of the microscopy technique used,[27] it might be possible 'to miss' the signal of interest.

Localisation of the probe in the bilayer

We have noted earlier that biexponential decays were observed for BODIPY in binary lipid–Chol mixtures and in single lipid bilayers when in the gel phase. This was attributed to the variations in the local viscosity of the environment of the rotor, *i.e.* the presence of at least two fractions of BODIPY in a bilayer (approximately 50 : 50, of *ca.* 160 cP (1.5 ns) and *ca.* 1300 cP (4.5 ns)). Such high heterogeneity is not surprising in a gel phase of lipids. Similarly, in the ternary mixtures the biexponential fitting of both the L_o and L_d decays was required, with about 10–15% of a fast ($\sim$1 ns) component. The value or the amplitude of this component did not change with lipid composition. The more dominant (85–90%) longer lifetime component (2–3.7 ns), on the other hand, significantly changed with lipid composition and it was that component that we interpreted as reflecting the viscosity change. Thus, we hypothesise that around 10–15% of the fluorophores are probably localised in such a way that the viscosity change in a bilayer does not alter their intramolecular rotation (*e.g.* lying parallel to the membrane surface). Ultimately, this lowers the average lifetime values and reduces the probe sensitivity to viscosity changes, see Table S1 (ESI†).

We have used quenching of BODIPY fluorescence with acrylamide to demonstrate that the rotor accessibility (and thus its position within the membrane leaflet) changed in the gel phase, compared to the liquid lipid phase, Fig. S8 (ESI†).

We have also used 2fFCS in GUVs containing DOPC/Chol (75/25) to directly probe the diffusion coefficient of the molecular rotor, as compared to four different labeled lipids or lipid tracers. We expected that any anomalies in our probe localisation will be reflected by a significantly different value of D, compared to commonly used bilayer probes.

Table 2 Diffusion coefficients of selected membrane dyes in DOPC/Chol (75/25) membranes measured by means of two-foci FCS

Label	D [μm^2 s^{-1}]	StDev [μm^2 s^{-1}]	N^a
BODIPY-FL-C_{12}	13.8	0.8	6
BODIPY-FL-DHPE	11.7	0.5	7
$DiOC_{18}$	9.4	0.7	7
BODIPY rotor	11.7	1.4	10

[a] The number of measurements performed.

For comparison we have selected a head labelled lipid (BODIPY-FL-DHPE), labelled dodecanoic acid (BODIPY-FL-C_{12}) and a two-chain lipid tracer ($DiOC_{18}$), Scheme 1. Table 2 gives the values of diffusion coefficients obtained. From these data it is clear that the diffusion coefficient of the BODIPY rotor matches well the diffusion coefficient of the head group labelled lipid molecule. This suggests that the translation diffusion of the rotor reflects the collective diffusion of the other lipid membrane components.

Conclusions

In this manuscript we have reported the first direct measurements of viscosity in model lipid bilayers, by means of detection of fluorescence lifetime of a molecular rotor. Specifically, we have investigated viscosity in mono-, binary and ternary lipid mixtures and studied the effect of temperature and lipid composition on the observed viscosity values. In view of the fact that our rotor can be used as a probe for live biological cells[7,8] we focused on aspects of membrane biophysics that are thought to accompany many important membrane associated processes, such as changes in the level of cholesterol, in saturated *versus* non-saturated lipid ratios and, importantly, the lipid phase.

We have demonstrated here that the level of cholesterol in the fluid binary and ternary lipid systems affects the rotor lifetime, and, consequently, the membrane viscosity at the location of the rotor. We have also established that the relationship between membrane viscosity and the diffusion coefficient (commonly measured by FCS) is not straightforward, since the diffusion in planar systems such as bilayers can reflect the changes in other parameters such as membrane thickness and/or hydrophobic mismatch.

Our results suggest that the BODIPY molecular rotor is most sensitive to the phase change in model membranes. This could be seen in all systems studied, from single-lipid experiments where the gel-to-L_d transition can be precisely detected, to ternary systems, where L_d and L_o phases can be clearly distinguished by the rotor lifetime and the corresponding viscosities measured. Thus, it could be expected that in cells the BODIPY rotor might be sensitive to the formation of lipid clusters with a higher level of lipid organisation (*e.g.* lipid rafts).

Finally, we have examined the dye localisation in the bilayer. On the basis of biexponential fluorescence decays observed in

some cases we can conclude that in these mixtures BODIPY is not distributed homogenously. This is particularly obvious in gel phases, where the more exposed (short lived) fraction of the BODIPY constitutes up to 50% of the fluorescence decay. However, both the fluorescence lifetime decays as well as the quenching experiments performed in liquid phases indicate that the BODIPY is deeply buried within the bilayer leaflet and its lifetime reflects the viscosity of the tail region of the bilayer. Notably, the fluorescence lifetime of the same rotor measured previously in internal membranes in live SK-OV-3 cells was 1.6 ± 0.2 or 2.0 ± 0.2 ns (monoexponential), depending on the cell domain examined.[7,8] These values match well the lifetimes detected here for liquid phases of DOPC and its mixtures with cholesterol and sphingomyelin. Our future efforts will concentrate on designing a BODIPY rotor which can be localised in the plasma membrane of cells.

Acknowledgements

MKK is thankful to the UK's Engineering and Physical Science Research Council (EPSRC) for the Career Acceleration Fellowship (EP/E038980/1). This work was supported in part by the EPSRC platform grant EP/G00465X/1. Support from the Czech Science Foundation *via* grant P208/12/G016 (AO, MH, MS) and the Ministry of Education, Youth and Sports of the Czech Republic *via* grant AVC-VTS LH13259 (JH) is acknowledged. MS is thankful for support from the Grant Agency of Charles University (grant No. 3130/2011). Moreover, MH acknowledges the Praemium Academie Award (Academy of Sciences of the Czech Republic).

Notes and references

1 E. Ikonen, *Curr. Opin. Cell Biol.*, 2001, **13**, 470.
2 Y. Chen, B. C. Lagerholm, B. Yang and K. Jacobson, *Methods*, 2006, **39**, 147.
3 G. J. Schutz, H. Schindler and T. Schmidt, *Biophys. J.*, 1997, **73**, 1073.
4 N. Kahya, D. Scherfeld, K. Bacia, B. Poolman and P. Schwille, *J. Biol. Chem.*, 2003, **278**, 28109.
5 J. Sankaran, X. K. Shi, L. Y. Ho, E. H. K. Stelzer and T. Wohland, *Opt. Express*, 2010, **18**, 25468.
6 (*a*) T. Wohland, X. K. Shi, J. Sankaran and E. H. K. Stelzer, *Opt. Express*, 2010, **18**, 10627; (*b*) J. Capoulade, M. Wachsmuth, L. Hufnagel and M. Knop, *Nat. Biotechnol.*, 2011, **29**, 835.
7 M. K. Kuimova, G. Yahioglu, J. A. Levitt and K. Suhling, *J. Am. Chem. Soc.*, 2008, **130**, 6672.
8 J. A. Levitt, M. K. Kuimova, G. Yahioglu, P. H. Chung, K. Suhling and D. Phillips, *J. Phys. Chem. C*, 2009, **113**, 11634.
9 M. A. Haidekker and E. A. Theodorakis, *Org. Biomol. Chem.*, 2007, **5**, 1669.
10 M. K. Kuimova, S. W. Botchway, A. W. Parker, M. Balaz, H. A. Collins, H. L. Anderson, K. Suhling and P. R. Ogilby, *Nat. Chem.*, 2009, **1**, 69.
11 M. K. Kuimova, *Phys. Chem. Chem. Phys.*, 2012, **14**, 12671.
12 E. P. Petrov and P. Schwille, *Biophys. J.*, 2008, **94**, L41.
13 T. Förster and G. Hoffmann, *Z. Phys. Chem.*, 1971, **75**, 63.
14 M. A. Haidekker, T. P. Brady, D. Lichlyter and E. A. Theodorakis, *J. Am. Chem. Soc.*, 2006, **128**, 398.
15 K. Akashi, H. Miyata, H. Itoh and K. Kinosita, *Biophys. J.*, 1996, **71**, 3242.
16 M. J. Hope, M. B. Bally, L. D. Mayer, A. S. Janoff and P. R. Cullis, *Chem. Phys. Lipids*, 1986, **40**, 89.
17 L. Beranova, J. Humpolickova, J. Sykora, A. Benda, L. Cwiklik, P. Jurkiewicz, G. Grobner and M. Hof, *Phys. Chem. Chem. Phys.*, 2012, **14**, 14516.
18 T. Dertinger, V. Pacheco, I. von der Hocht, R. Hartmann, I. Gregor and J. Enderlein, *ChemPhysChem*, 2007, **8**, 433.
19 M. A. H. Alamiry, A. C. Benniston, G. Copley, K. J. Elliott, A. Harriman, B. Stewart and Y. G. Zhi, *Chem. Mater.*, 2008, **20**, 4024.
20 J. Sykora, V. Mudogo, R. Hutterer, M. Nepras, J. Vanerka, P. Kapusta, V. Fidler and M. Hof, *Langmuir*, 2002, **18**, 9276.
21 D. Hoekstra and S. C. D. van IJzendoorn, *Curr. Opin. Cell Biol.*, 2000, **12**, 496.
22 A. Benda, M. Benes, V. Marecek, A. Lhotsky, W. T. Hermens and M. Hof, *Langmuir*, 2003, **19**, 4120.
23 P. G. Saffman and M. Delbrück, *Proc. Natl. Acad. Sci. U. S. A.*, 1975, **72**, 3111.
24 J. Pan, S. Tristram-Nagle and J. F. Nagle, *Phys. Rev. E: Stat., Nonlinear, Soft Matter Phys.*, 2009, **80**, 021931.
25 S. L. Veatch and S. L. Keller, *Biochim. Biophys. Acta, Mol. Cell Res.*, 2005, **1746**, 172.
26 A. K. Smith and J. H. Freed, *J. Phys. Chem. B*, 2009, **113**, 3957.
27 C. Eggeling, C. Ringermann, R. Medda, G. Schwarzmann, K. Sandhoff, S. Polyakova, V. N. Belov, B. Hein, C. von Middendorff, A. Schoenle and S. W. Hell, *Nature*, 2009, **457**, 1159.